A bimetallic nanocoral Au decorated with Pt nanoflowers (bio)sensor for H$_2$O$_2$ detection at low potential

Gabriella Sanzò [a,b,1], Irene Taurino [a,1], Francesca Puppo [a], Riccarda Antiochia [b], Lo Gorton [c], Gabriele Favero [b], Franco Mazzei [b], Sandro Carrara [a], Giovanni De Micheli [a,*]

[a] Laboratory of Integrated Systems, EPFL – École Polytechnique Fédérale de Lausanne, 1015 Lausanne, Switzerland
[b] Biosensors Laboratory, Department of Chemistry Drug Technologies, Sapienza University of Rome, P.le Aldo Moro, 5-00185 Roma, Italy
[c] Department of Analytical Chemistry/Biochemistry, P.O. Box 124, 221 00 Lund, Sweden

ARTICLE INFO

ABSTRACT

In this work, we have developed for the first time a method to make novel gold and platinum hybrid bimetallic nanostructures differing in shape and size. Au-Pt nanostructures were prepared by electrodeposition in two simple steps. The first step consists of the electrodeposition of nanocoral Au onto a gold substrate using hydrogen as a dynamic template in an ammonium chloride solution. After that, the Pt nanostructures were deposited onto the nanocoral Au organized in pores. Using Pt (II) and Pt (IV), we realized nanocoral Au decorated with Pt nanospheres and nanocoral Au decorated with Pt nanoflowers, respectively. The bimetallic nanostructures showed better capability to electrochemically oxidize hydrogen peroxide compared with nanocoral Au. Moreover, Au-Pt nanostructures were able to lower the potential of detection and a higher performance was obtained at a low applied potential. Then, glucose oxidase was immobilized onto the bimetallic Au-Pt nanostructure using cross-linking with glutaraldehyde. The biosensor was characterized by chronoamperometry at +0.15 V *vs.* Ag pseudo-reference electrode (PRE) and showed good analytical performances with a linear range from 0.01 to 2.00 mM and a sensitivity of 33.66 μA/mM cm^2. The good value of K$_m^{app}$ (2.28 mM) demonstrates that the hybrid nanostructure is a favorable environment for the enzyme. Moreover, the low working potential can minimize the interference from ascorbic acid and uric acid as well as reducing power consumption to effect sensing. The simple procedure to realize this nanostructure and to immobilize enzymes, as well as the analytical performances of the resulting devices, encourage the use of this technology for the development of biosensors for clinical analysis.

© 2017 Published by Elsevier Inc.

1. Introduction

Precision medicine relies on the accurate acquisition of large data sets through biosensors as well as data processing including a variety of methods, among which machine learning is of paramount importance. The acquisition of large-scale biomedical data, often performed in real time, poses a strong challenge to the design of the front-end sensing structure and circuitry, because of the requirements of being accurate and achieved within a power-consumption envelope. Within this perspective, the co-design of sensing structures, circuits and data processing means is essential. Here we show how to nanostructure electrodes to achieve biosensing with low power consumption.

Electrochemical biosensors based on the detection of hydrogen peroxide (H$_2$O$_2$) were one of the very first ones because H$_2$O$_2$ is the one of the main products in many reactions catalysed by oxidases. In the last years the use of nanostructured-based modified electrodes able to drastically lower the applied potential gave new interest on the use of these biodevices [1,2]. In fact, although the first generation biosensors are still widely used, the principal drawback is that H$_2$O$_2$ is sensed at a high potential (+0.70 V *vs.* Ag|AgCl) on most electrode materials and possible interfering components present in biological fluids such as ascorbic acid (AA), uric acid (UA) and acetaminophen (APAP) can be oxidized at this high potential and generate a faradic current that interferes in the measurement of the analyte [3,4]. In order to minimize the oxidation of interfering components, it is preferred to work in a potential range from −0.2 to +0.15 V *vs.* Ag|AgCl [5,6]. To overcome the problem of interferences in a real matrix, the research was focused on developing different strategies. The most popular approach reported in

the literature, requires a redox mediator such as Prussian Blue to modify the electrode surface and, in this case, H_2O_2 can be sensed at a low potential (around +0.0 V) avoiding the interference of electroactive molecules [7–9]. A possible alternative is to realize a bienzymatic biosensor with the incorporation of peroxidase, which can communicate through direct electron transfer between the active site of the enzyme and the electrode surface [10–12]. Despite the advantage of these approaches, different disadvantages arise. It is known that many enzymes require neutral or alkaine pH but at this pH value Prussian Blue is unstable and will deteriorate [7]. The main disadvantages of the bienzymatic biosensor are the instability due to the presence of two enzymes and the difficulty in the binding of peroxidases onto solid surfaces [3]. With the advent of nanotechnology, an interest was focused on developing new nanomaterials and to employ them for an improved sensor sensitivity and for a preservation of the native structure of the enzyme when immobilized onto the electrode surface [18–25]. In particular, more recent studies demonstrate that the electrode modification with metal nanoparticles such as gold [4,13,14] or platinum [15–17] decreases the overpotential for the detection of H_2O_2. Nanostructures based on transition metals such as Au and Pt, thanks to their capability to enhance the electrocatalytic activity towards H_2O_2 oxidation, have been incorporated into electrode surfaces to make biosensors [26–30]. Different studies demonstrated that the combination of two metallic nanostructures generates a new structure with different chemical and physical properties that were not observed by using one single metallic nanocatalyst alone [31–33]. According to the literature, AuPt hybrid nanostructures have become more attractive thanks to the synergistic catalytic effect and an excellent resistance to poisoning [34–39]. Different strategies to realize AuPt hybrid structures are reported in literature such as the dealloying method that involves multiple steps [40,41].

In this work we present a simple method for the development of Au-Pt bimetallic nanostructures, by using an electrodeposition method thus obtaining several advantages compared to chemical and physical techniques such as the purity of the new nanostructures and the good control of the dimension of the nanofeatures [42–44]. We demonstrated the synergic effect of Au in combination with Pt to reduce the detection potential of H_2O_2. In particular, we realized, to the best of our knowledge and for the first time, two different AuPt hybrid nanostructures consisting of Au nanocorals decorated with Pt nanoflowers ($Au_{Nc}Pt_{Nf}$) and of Au nanocorals decorated with Pt nanospheres ($Au_{Nc}PtN_{sph}$). The realization of these structures required only two simple electrodeposition steps. The resulting structures were firstly characterized by scanning electron microscopy (SEM). A chronoamperometric study of H_2O_2 detection using bare Au and Pt, Au and Pt nanostructures and AuPt hybrid nanocomposites was performed at different potentials. $Au_{Nc}Pt_{Nf}$ exhibited the best performance for H_2O_2 detection. Successively, glucose oxidase (GOx) was utilized as a model oxidase and a first generation glucose biosensor was fabricated immobilizing the enzyme by cross-linking with glutaraldehyde [45] onto an $Au_{Nc}Pt_{Nf}$ modified electrode. The realized glucose biosensor was characterized by chronoamperometry at +0.15 V vs. Ag PRE and the effect of interfering species (AA, UA, APAP) was also evaluated.
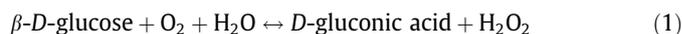
2. Results and discussion

2.1. Morphological characterization

In Fig. 1 SEM images of the various Au-Pt hybrid nanostructures are shown. With the first electrodeposition step, a layer of Au nanocorals was formed, which is organized in pores (Figs. 1(a and b)). The morphological characterization of the Au nanocorals

was described in our previous work [46]. Au nanocorals present different sites for the attachment of either Pt nanoflowers or Pt nanospheres realized in the second electrodeposition step. In our previous work [47], we demonstrated that the composition of the solution and the applied potential during the electrodeposition are important parameters to obtain Pt nanostructures differing in shape and size. In the magnification of Fig. 1a, Au nanocorals obtained from $HAuCl_4$-containing solutions is shown. Fig. 1b shows Pt nanoflowers obtained with H_2PtCl_6 and uniformly electrodeposited outside of the Au pores. Similarly, also Pt nanospheres obtained with K_2PtCl_4 were only formed outside of the Au pores as shown in the magnification of Fig. 1c.

2.2. Electrooxidation of H_2O_2

Glucose can be indirectly determined by sensing H_2O_2 product of the following enzymatic reaction [8]

$$\beta\text{-}D\text{-glucose} + O_2 + H_2O \leftrightarrow D\text{-gluconic acid} + H_2O_2 \tag{1}$$

To evaluate the catalytic activity toward H_2O_2 oxidation, a series of measurements were carried out using the different modified electrodes described above. In the first experiment, the amperometric response to 20 μM H_2O_2 was evaluated as a function of the applied potential using different surfaces. The potential was varied from +0.7 to +0.2 V vs. Ag PRE and the results are shown in Fig. 2. It can be seen that for a bare Au electrode, the current response increases with an increase in the applied potential from +0.3 to +0.7 V and no response was obtained at a potential lower than +0.3 V. With Au nanocorals, the amperometric response was observed also at +0.2 V and the current increased with an increase in potential from +0.2 to +0.7 V. Interestingly, with both bimetallic nanostructures, not only the current reaches a higher value but the amperometric response, obtained in 100 s, increases by decreasing the applied potential from +0.7 to +0.2 V. These results suggest that the capability to improve the amperometric performance with a reduction in the applied potential, could be due not only to the excellent catalytic properties of Pt and the realized nanostructures but also to the synergic effect due to the combination of Au and Pt nanostructures. Moreover, if comparing the results of the two different bimetallic nanostructures ($Au_{Nc}Pt_{Nf}$ and $Au_{Nc}PtN_{sph}$), it should be noted that although the trend is the same, Pt nanoflowers have a shape that give a major contribute to enhance the catalytic performance toward H_2O_2 detection compared to Pt nanospheres. The explanation might be that Pt nanoflowers exhibit a more nanostructured surface than Pt nanospheres. The higher current acquired with $Au_{Nc}Pt_{Nf}$ than $Au_{Nc}PtN_{sph}$ is due to a major surface area to electrooxidize H_2O_2. Since our goal is to realize a biosensor with high performance, we have chosen to work with $Au_{Nc}Pt_{Nf}$ in the successive study.

2.3. Effect of the potential on the sensitivity

The response to different concentrations of H_2O_2 was investigated in order to calculate the sensitivity for H_2O_2 at different applied potentials using the three different steps involved in making the $Au_{Nc}Pt_{Nf}$. The calibration experiments were carried out in the concentration range between 20 μM and 100 μM at different potentials using Au bare, Au nanocorals and $Au_{Nc}Pt_{Nf}$; the response currents obtained are shown in Fig. 3(a–c). The trends confirm the data obtained in the previous experiments. With Au bare, the sensitivity increased with an increase in applied potential. With Au nanocorals the sensitivity is higher than that one obtained with Au bare and the sensitivity increased with an increase in applied potential. As expected, the best results have been achieved with the bimetallic nanostructures, where the sensitivity increased with a decrease in the applied potential, suggesting that the combina-
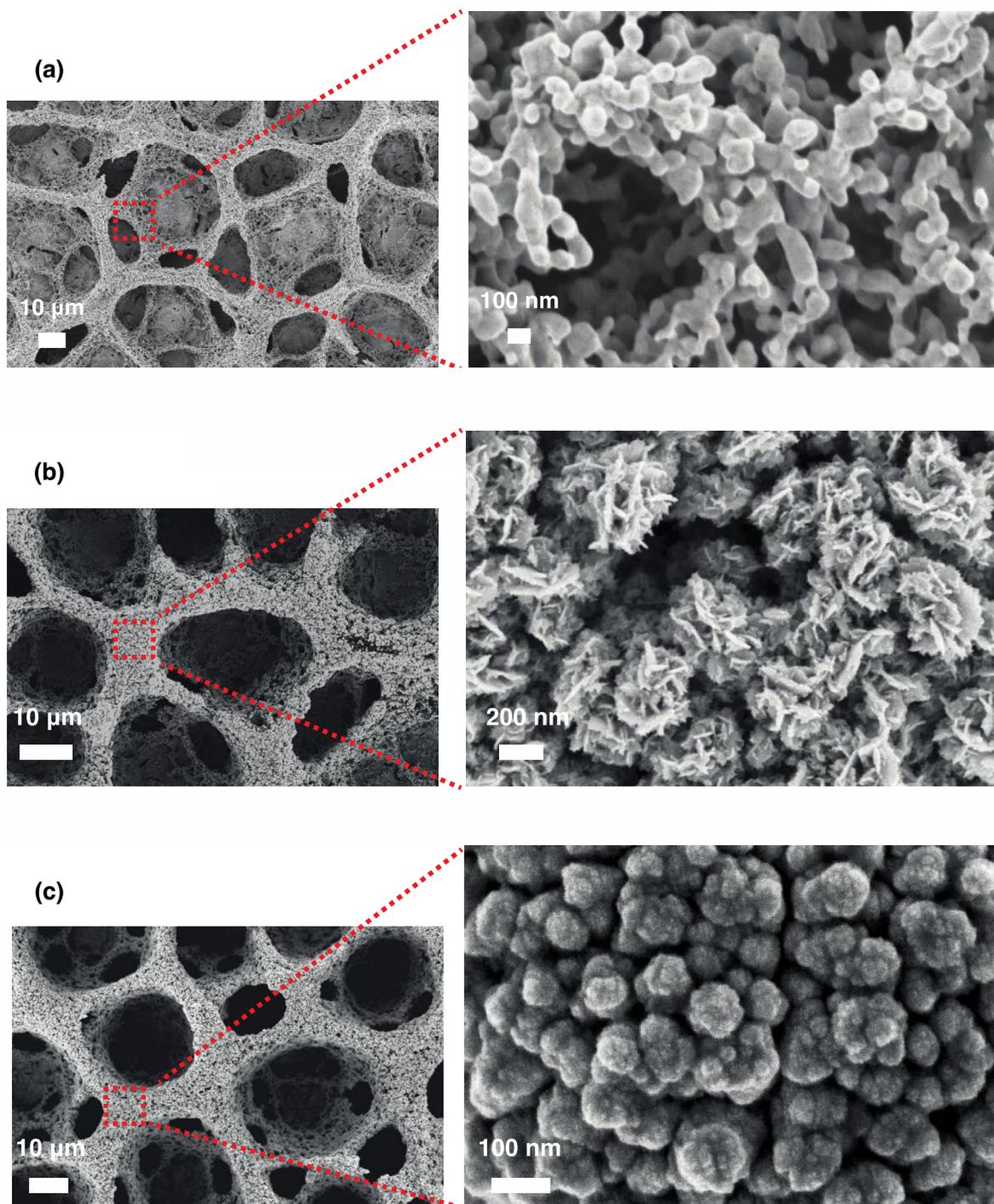
Fig. 1. SEM images of (a) Au nanocorals, (b) Au nanocorals with Pt nanoflowers (−1 V for 90 s from tetravalent Pt) and (c) with Pt nanospheres (−0.2 V for 200 s from divalent Pt).

tion of Pt with Au can generate a new structure with unique properties. It was proven that combining nanostructures of Pt and of other metals further reduces poisoning issues and further favors the detection of small molecules at even lower potential than using monometallic Pt nanomaterials [48]. The improvement in electrocatalysis by coupling Pt with other metals could be due to the higher/lower electronegativity of the second metal that could cause an increase/decrease in the amount of charge being trans-

ferred from Pt to the second metal [40]. Moreover, a particular arrangement of surface atoms of the two metals suppresses adsorbed poisonous species on surface-active sites of Pt. The shift of the electron density of the d-band of Pt in the presence of another metal reduces the strength of the molecular adsorption on Pt and, therefore, lower the detection potential [49,50]. Note that the main factor that contributes to lowering the potential, is not the higher surface area of the nanostructures but the particular
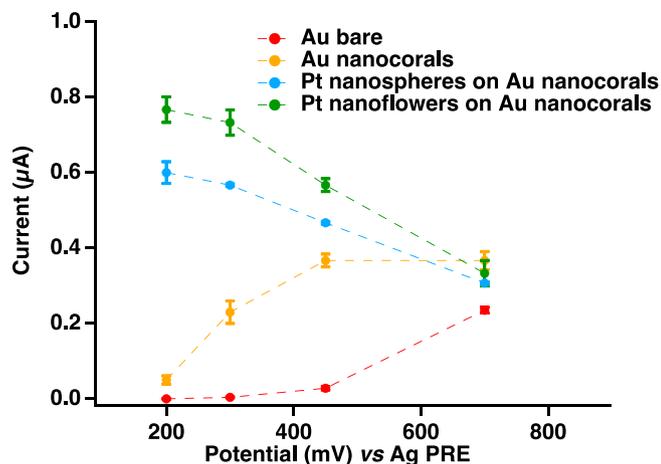
Fig. 2. Effect of applied potential on the amperometric response to 20 μM H2O2 at (red) bare Au, (orange) Au nanocorals, (green) $Au_{Nc}Pt_{Nf}$ and (blue) $Au_{Nc}Pt_{Nsph}$ electrodes. Amperometric measurements were performed at various levels of the applied potential in stirred 0.01 M PBS pH 7.4 solution by injecting 20 μM H2O2. (For interpretation of the references to colour in this figure legend, the reader is referred to the web version of this article.)

combination of two different metals. This hypothesis was confirmed with Au nanocorals, where the surface area increased and the amperometric performance was higher than that of Au bare but the behavior at the different potentials is the same. The new structures combining the advantages of Au nanocorals (high surface area, electrocatalytic activity) with those of Pt nanoflowers (nano size effect, good biocompatibility for enzyme, high surface area, high catalytic activity) are an excellent platform to immobilize GOx and to perform measurements at a low potential.

2.4. Influence of applied potential on biosensor response

The effect of applied potential on the amperometric response of the $Au_{Nc}Pt_{Nf}$/GOx biosensor was also investigated. The measurements were performed under stirred conditions in 0.01 M phosphate buffer at pH 7.4 by injection of 0.1 mM glucose after baseline stabilization for each potential. With the biosensor, a larger range potential was investigated and the amperometric response of the biosensor to glucose versus applied potential in the range of +0.10 to +0.70 V vs. Ag PRE is illustrated in Fig. 4. The results showed that the applied potential had a significant effect on the response of the biosensor. Also in this case, a higher response was obtained at low potential values. The biosensor presented the highest response current at +0.15 V; that means that this enzyme modified electrode is ideal for glucose detection at a low potential. Since a high current response was obtained at a low potential and that the interference of AA and UA should be minimized, +0.15 V was selected for characterization of the realized biosensor.

2.5. Biosensor performance

Fig. 5 shows the current-time response of the $Au_{Nc}Pt_{Nf}$/GOx biosensor on successive additions of glucose in a stirred solution of PBS at the applied potential of +0.15 V vs. Ag PRE. The inset of Fig. 5 shows the amperometric current response of the biosensor as a function of glucose concentration. The calibration curve is linear in the range between 0.01 and 2.0 mM. The apparent
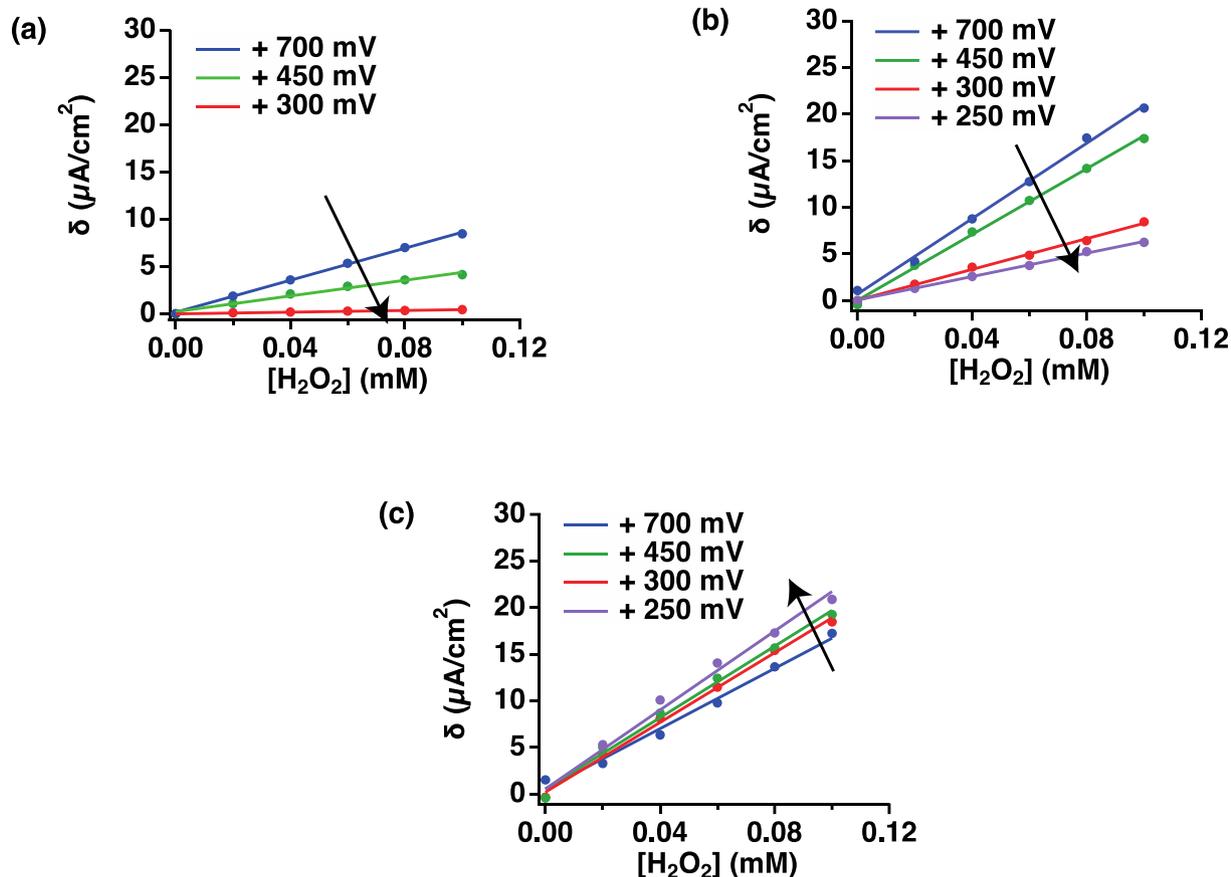

Fig. 3. Effect of the applied potential on the sensitivity by using (a) Au bare, (b) Au nanocorals and (c) $Au_{Nc}Pt_{Nf}$.

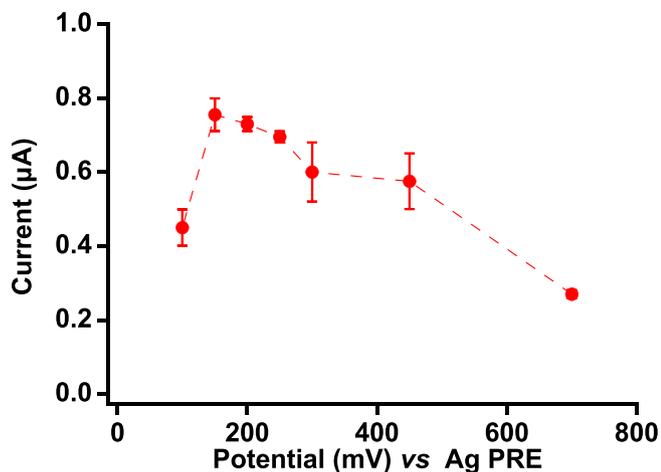**Fig. 4.** Effect of applied potential on the amperometric response at $Au_{Nc}Pt_{Nf}$ electrode towards the detection of 1 mM glucose.

Michaelis-Menten constant (K_m^{app}) of the biosensor was calculated to be 2.28 mM according to the electrochemical Lineweaver-Burk form, the relationship between the reciprocal of current and the reciprocal of glucose concentration. This value of K_m^{app} is lower than those found with other biosensors based on GOx (see Table 1). The morphological characteristics of the electrode surface allow an optimal distribution of the enzyme thus making it more accessible to the substrate (glucose). The biosensor sensitivity (determined from the slope of the initial linear part of the calibration) was 33.66 μA/mM cm^2.

Table 1 compares the analytical performances of different GOx biosensors with those obtained using $Au_{Nc}Pt_{Nf}$/GOx biosensor. It can be seen that the $Au_{Nc}Pt_{Nf}$-modified biosensor showed the best compromise between high sensitivity and low potential applied.

2.6. Interference study

The detection at a low potential can minimize the contributions from interfering components present in a real matrix. In this way, the effect of AA, UA and APAP in physiological concentration upon the response of the $Au_{Nc}Pt_{Nf}$/GOx biosensor was investigated at the operation potential of +0.15 V vs. Ag PRE under stirred conditions in a 0.01 M phosphate buffer. As is shown in Fig. 6, the injection of glucose generated an increment in the response current whereas with the addition of UA and AA no noticeable increase in current was observed (Fig. 6(a)). Also the addition of APAP did not cause any effect on the response of the biosensor (Fig. 6(b)). These values showed that this low potential can avoid the interference of AA, UA and APAP and that the proposed biosensor could be utilized in the analysis of a real matrix.

3. Conclusions

A new bimetallic nanocomposite was obtained in two simple steps by an electrodeposition method. The results reported in this work showed that a new nanocomposite with unique and attractive properties was fabricated thus constituting the basis for new electrochemical biosensors for biomedical applications. The realized bimetallic nanocomposite presents new and interesting properties with a higher sensitivity and stability but especially the possibility to lower the detection potential of H_2O_2. The combination of Au nanocoral and Pt nanoflowers not only increased the electroactive surface area but improved the amperometric detection of glucose at a low potential. Avoiding of interference of AA, UA, and APAP suggests that the proposed biosensor could be applied in analysis of biological fluids.

4. Materials and methods

4.1. Chemicals

Gold (III) chloride hydrate from Sigma and ammonium chloride were purchased from BioChemica. Chloroplatinic acid hexahydrate (H_2PtCl_6 $6H_2O$), H_2SO_4 (95–98%), potassium chloride (minimum 99.0%), ascorbic acid, uric acid, potassium hexacyanoferrate (III) (99%) and D-(+)-glucose, glutaraldehyde solution, grade II, 25% were purchased from Sigma. Potassium chloroplatinic acid (K_2-$PtCl_4$) was acquired from Fisher-Sci. Glucose oxidase (GOx, EC 1.1.3.4, from *Aspergillus niger*) grade I, 2 MU/5.06 g was obtained
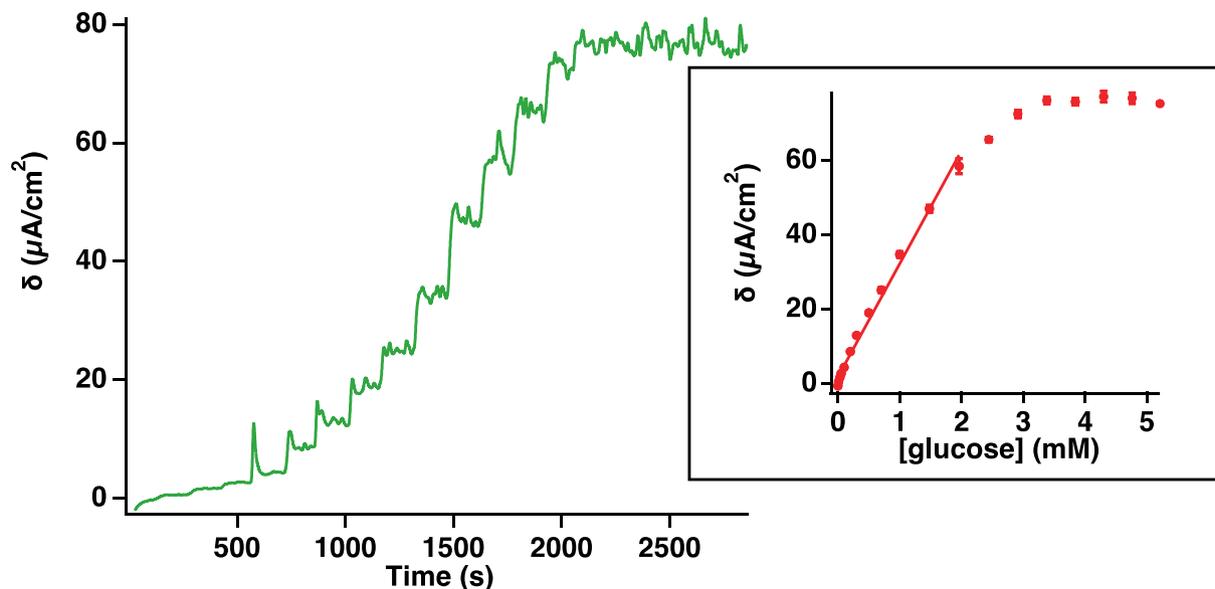

Fig. 5. Amperometric response obtained to successive additions of glucose in a stirred 10 ml solution of PBS 0.01 M pH 7.4 at +0.15 V (vs. Ag PRE) using $Au_{Nc}Pt_{Nf}$/GOx biosensor. The inset shows the amperometric current density response of the biosensor as a function of glucose concentration.

Table 1
Comparison of electrochemical performances of some 1st generation glucose biosensors.

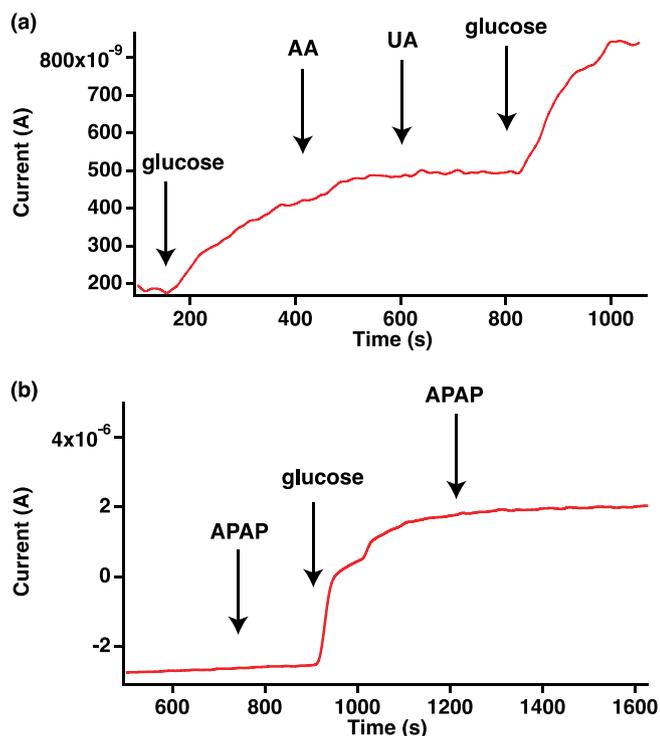| GOx biosensors	Applied potential (V)	Linear range (mM)	Sensitivity	K_m^{app} (mM)	Ref.
GOx/Au-PtNPs/CNTs/CS/GCE	+0.1 vs Ag|AgCl	0.001–7	8.53 μA mM^{-1}	5.20	[37]
Pt/PVF-Au-GOx	+0.6 vs SCE	1–36	4.17 μA mM^{-1} cm^{-2}	–	[51]
GOx–Au$_{coll}$–CNT–Teflon	+0.5 vs Ag|AgCl	0.05–1	37.14 μA mM^{-1} cm^{-2}	14.9	[52]
Pt/Rh/AuNP-GOx-Nafion	+0.35 vs Ag|AgCl	0.05–15	68.1 μA mM^{-1} cm^{-2}	–	[53]
GOx/Au$_{nano}$/Pt$_{nano}$/CNT/gold	+0.6 vs SCE	0.5–16.5	–	10.73	[54]
GOD/Pt/OMC/Au	−0.1 vs Ag|AgCl	0.05–3.7	0.38 μA mM^{-1}	2.18	[55]
Au$_{Nc}$Pt$_{Nf}$/GOx	+0.15 vs Ag PRE	0.01–2	33.66 μA mM^{-1} cm^{-2}	2.28	This work

Fig. 6. Current-time response curve of the Au$_{Nc}$Pt$_{Nf}$/GOx biosensor to several interfering species in PBS 0.01 M pH 7.4 at +0.15 V (vs. Ag PRE). (a) 0.5 mM glucose, 0.1 M AA, 0.01 M UA and (b) 1 mM glucose, APAP 0.015 M and 0.045 M first and second injection, respectively.

from Roche Diagnostics. Phosphate buffer saline from Sigma at pH 7.4 was used to prepare all the solutions.

4.2. Electrodeposition of Pt nanostructures onto Au nanocoral

Au nanocoral-based electrode was developed according to the procedure reported in our previous work [46]. Pt nanoflowers were electrodeposited onto the Au nanocoral surface using a three-electrode configuration with Au nanocorals as working electrode, carbon as counter and Ag PRE. Before Pt deposition, the Au nanocoral surface was cleaned by following the method reported in [56]. A solution consisting of 25 mM H$_2$PtCl$_6$ or K$_2$PtCl$_4$ and 50 mM H$_2$SO$_4$ was used for electrodeposition of Pt nanoflowers and nanospheres, respectively [47]. The prepared bimetallic nanostructure was cleaned in 100 mM H$_2$SO$_4$ by applying a potential of +2.0 V vs. Ag PRE for 120 s [57].

4.3. Surface characterization

The morphological surface was characterized before and after the electrodeposition of Pt nanoflowers and Pt nanospheres onto Au nanocorals by SEM using a Zeiss Merlin Microscope.

4.4. Biosensor assembly

A mixture of glutaraldehyde 2.5% (50 μl) with 10 mM PBS (950 μl) and 15 mg of GOx was prepared. After homogenization with vortex mixing, 10 μl of the enzymatic solution was spread on the Au$_{Nc}$Pt$_{Nf}$ electrodes. In order to obtain cross-linking between glutaraldehyde and enzyme, the biosensors were kept overnight at 4 °C before the experiments.

4.5. Electrochemical measurements

A Potentiostat with NOVA software (Eco Chemie, Utrecht, The Netherlands) with a conventional three-electrode configuration was used to perform cyclic voltammetry (CV) and chronoamperometric measurements.

Screen-Printed Electrodes (SPEs) (Metrohm) with a gold working electrode (4 mm diameter), carbon counter electrode and Ag PRE were used. Cyclic voltammetric experiments were carried out in a static electrochemical cell, while amperometric experiments were carried out under stirring conditions with a successive addition of H$_2$O$_2$ or glucose to the cell. All potentials given were referred to Ag PRE reference electrode. Measurements were carried out under aerobic conditions at room temperature in 0.01 M phosphate buffer at pH 7.4.

Acknowledgements

References

[1] S.X. Xu, J.L. Li, Z.L. Zhou, C.X. Zhang, A third-generation hydrogen peroxide biosensor based on horseradish peroxidase immobilized by sol–gel thin film on a multi-wall carbon nanotube modified electrode, Anal. Methods 6 (2014) 6310–6315.
[2] R.E. Sabzi, F. Rasouli, F. Kheiri, Amperometric hydrogen peroxide biosensor based on horseradish peroxidase entrapped in titania sol-gel film on screen-printed electrode, Am. J. Anal. Chem. 4 (2013) 607–615.
[3] M. Raicopol, A. Prună, C. Damian, L. Pilan, Functionalized single-walled carbon nanotubes/polypyrrole composites for amperometric glucose biosensors, Nanoscale Res. Lett. 8 (2013) 316.
[4] Z. Wen, S. Ci, J. Li, Pt Nanoparticles inserting in carbon nanotube arrays: nanocomposites for glucose biosensors, J. Phys. Chem. C 113 (2009) 13482–13487.
[5] D. Pan, J. Chen, L. Nie, W. Tao, S. Yao, An amperometric glucose biosensor based on poly(o-aminophenol) and Prussian blue films at platinum electrode, Anal. Biochem. 324 (2004) 115–122.
[6] L. Gorton, E. Csöregi, E. Dominguez, J. Emnéus, G. Jönsson-Pettersson, G. Marko-Varga, B. Persson, Selective detection in flow analysis based on the combination of immobilized enzymes and chemically modified electrodes, Anal. Chim. Acta 250 (1991) 203–248.
[7] F. Ricci, G. Palleschi, Sensor and biosensor preparation, optimisation and applications of Prussian Blue modified electrodes, Biosens. Bioelectron. 21 (2005) 389–407.
[8] J. Wang, Electrochemical glucose biosensors, Chem. Rev. 108 (2008) 814–825.
[9] I.L. de Mattos, L. Gorton, T. Ruzgas, Sensor and biosensor based on Prussian Blue modified gold and platinum screen printed electrodes, Biosens. Bioelectron. 18 (2003) 193–200.

[10] A.S. Santos, N. Durán, L.T. Kubota, Biosensor for H₂O₂ response based on horseradish peroxidase: effect of different mediators adsorbed on silica gel modified with niobium oxide, Electroanalysis 17 (2005) 1103–1111.

[11] T. Ruzgas, E. Csöregi, J. Emnéus, L. Gorton, G. Marko-Varga, Peroxidase-modified electrodes: fundamentals and application, Anal. Chim. Acta 330 (1996) 123–138.

[12] L. Gorton, G. Bremle, E. Csöregi, G. Jönsson-Pettersson, B. Persson, Amperometric glucose sensors based on immobilized glucose-oxidizing enzymes and chemically modified electrodes, Anal. Chim. Acta 249 (1991) 43–54.

[13] V.V. Shumyantseva, S. Carrara, V. Bavastrello, D.J. Riley, T.V. Bulko, K.G. Skryabin, Direct electron transfer between cytochrome P450scc and gold nanoparticles on screen-printed rhodium-graphite electrodes, Biosens. Bioelectron. 21 (2005) 217–222.

[14] A. Wittstock, V. Zielasek, J. Biener, C.M. Friend, M. Bäumer, Nanoporous gold catalysts for selective gas-phase oxidative coupling of methanol at low temperature, Science 15 (2010) 319–322.

[15] H. Tang, J. Chen, S. Yao, L. Nie, G. Deng, Y. Kuang, Amperometric glucose biosensor based on adsorption of glucose oxidase at platinum nanoparticle-modified carbon nanotube electrode, Anal. Biochem. 331 (2004) 89–97.

[16] Z. Miao, D. Zhang, Q. Chen, Non-enzymatic hydrogen peroxide sensors based on multi-wall carbon nanotube/Pt nanoparticle nanohybrids, Materials 7 (2014) 2945–2955.

[17] G. Yu, W. Wu, X. Pan, Q. Zhao, X. Wei, Q. Lu, High sensitive and selective sensing of hydrogen peroxide released from pheochromocytoma cells based on Pt-Au bimetallic nanoparticles electrodeposited on reduced graphene sheets, Sensors 15 (2015) 2709–2722.

[18] J. Xie, S. Wang, L. Aryasomayajula, V.K. Varadan, Platinum decorated carbon nanotubes for highly sensitive amperometric glucose sensing, Nanotechnology 18 (2007) 065503.

[19] P. Bollella, G. Fusco, C. Tortolini, G. Sanzò, G. Favero, L. Gorton, R. Antiochia, Beyond graphene: electrochemical sensors and biosensors for biomarkers detection, Biosens. Bioelectron. (2016), http://dx.doi.org/10.1016/j.bios.2016.03.068.

[20] C. Shan, H. Yang, D. Han, Q. Zhang, A. Ivaska, L. Niu, Graphene/AuNPs/chitosan nanocomposites film for glucose, Biosensing Biosens. Bioelectron. 25 (2010) 1070–1074.

[21] K. Kerman, M. Saito, S. Yamamura, Y. Takamura, E. Tamiya, Nanomaterial-based electrochemical biosensors for medical applications, TrAC Trends Anal. Chem. 27 (2008) 585–592.

[22] G. Favero, G. Fusco, F. Mazzei, F. Tasca, R. Antiochia, Electrochemical characterization of graphene and MWCNT screen-printed electrodes modified with AuNPs for laccase biosensor development, Nanomaterials 5 (2015) 1995–2006.

[23] M. Carbone, L. Gorton, R. Antiochia, An overview of the latest graphene-based sensors for glucose detection: the effects of graphene defects, Electroanalysis 27 (2015) 16–31.

[24] P. Bollella, F. Mazzei, G. Favero, G. Fusco, R. Ludwig, L. Gorton, R. Antiochia, Improved DET communication between cellobiose dehydrogenase and a gold electrode modified with a rigid self-assembled monolayer and green metal nanoparticles: the role of an ordered nanostructuration, Biosens. Bioelectron. (2016), http://dx.doi.org/10.1016/j.bios.2016.08.027.

[25] F. Tasca, R. Ludwig, L. Gorton, R. Antiochia, Determination of lactose by a novel third generation biosensor based on a cellobiose dehydrogenase and aryl diazonium modified single wall carbon nanotubes electrode, Sens. Actuators B 177 (2013) 64–69.

[26] H. Zhang, W. Zhou, Y. Du, P. Yang, C. Wang, One-step electrodeposition of platinum nanoflowers and their high efficient catalytic activity for methanol electro-oxidation, Electrochem. Commun. 12 (2010) 882–885.

[27] A. Ott, L.A. Jones, S.K. Bhargava, Direct electrodeposition of porous platinum honeycomb structures, Electrochem. Commun. 13 (2011) 1248–1251.

[28] Y. Du, X.L. Luo, J.J. Xu, H.Y. Chen, A simple method to fabricate a chitosan-gold nanoparticles film and its application in glucose biosensor, Bioelectrochemistry 70 (2007) 342–347.

[29] H.C. Liu, C.C. Tsai, G.J. Wang, Glucose biosensors based on a gold nanodendrite modified screen-printed electrode, Nanotechnology 24 (2013) 215101.

[30] I. Taurino, G. Sanzò, R. Antiochia, C. Tortolini, F. Mazzei, G. Favero, G. De Micheli, S. Carrara, Recent advances in third generation biosensors based on Au and Pt nanostructured electrodes, TrAC Trends Anal. Chem. 79 (2016) 151–159.

[31] S. Upadhyay, G.R. Rao, M.K. Sharma, B.K. Bhattacharya, V.K. Rao, R. Vijayaraghavan, Immobilization of acetylcholineesterase–choline oxidase on a gold–platinum bimetallic nanoparticles modified glassy carbon electrode for the sensitive detection of organophosphate pesticides, carbamates and nerve agents, Biosens. Bioelectron. 25 (2009) 832–838.

[32] J. Jia, L. Cao, Z. Wang, Platinum-coated gold nanoporous film surface: Electrodeposition and enhanced electrocatalytic activity for methanol oxidation, Langmuir 24 (2008) 5932–5936.

[33] S. Thiagarajan, S.M. Chen, Applications of nanostructured Pt-Au hybrid film for the simultaneous determination of catecholamines in the presence of ascorbic acid, J. Solid State Electrochem. 13 (2009) 445–453.

[34] Y. Song, Y. Ma, Y. Wang, J. Di, Y. Tu, Electrochemical deposition of gold–platinum alloy nanoparticles on an indium tin oxide electrode and their electrocatalytic applications, Electrochim. Acta 55 (2010) 4909–4914.

[35] F. Xiao, F. Zhao, Y. Zhang, G. Guo, B. Zeng, Ultrasonic electrodeposition of gold–platinum alloy nanoparticles on ionic liquid-chitosan composite film and their application in fabricating nonenzyme hydrogen peroxide sensors, J. Phys. Chem. C 113 (2009) 849–855.

[36] W. He, X. Wu, J. Liu, X. Hu, K. Zhang, S. Hou, W. Zhou, S. Xie, Design of AgM bimetallic alloy nanostructures (M=Au, Pd, Pt) with Tunable morphology and peroxidase-like activity, Chem. Mater. 22 (2010) 2988–2994.

[37] X. Kang, Z. Mai, X. Zou, P. Cai, J. Mo, A novel glucose biosensor based on immobilization of glucose oxidase in chitosan on a glassy carbon electrode modified with gold–platinum alloy nanoparticles/multiwall carbon nanotubes, Anal. Biochem. 369 (2007) 71–79.

[38] L. Gorton, G. Jönsson, A glucose sensor based on the adsorption of glucose on a palladium/gold modified carbon electrode, J. Molecular Cat. 38 (1986) 157–159.

[39] L. Gorton, A carbon electrode sputtered with palladium and gold for the amperometric detection of hydrogen peroxide, Anal. Chim. Acta 178 (1985) 247–253.

[40] Y. Li, Y.Y. Song, C. Yang, X.H. Xia, Hydrogen bubble dynamic template synthesis of porous gold for nonenzymatic electrochemical detection of glucose, Electrochem. Commun. 9 (2007) 981–988.

[41] R. Zhang, H. Olin, Porous gold films – a short review on recent progress, Materials 7 (2014) 3834–3854.

[42] S. Cherevko, C.H. Chung, Direct electrodeposition of nanoporous gold with controlled multimodal pore size distribution, Electrochem. Commun. 13 (2011) 16–19.

[43] H. Zhang, F. Jiang, R. Zhou, Y. Du, P. Yang, C. Wang, J. Xu, Effect of deposition potential on the structure and electrocatalytic behavior of Pt micro/nanoparticles, Int. J. Hydrogen Energy 36 (2011) 15052–15059.

[44] Y. Zhang, M. Janyasupab, C.W. Liu, P.Y. Lin, K.W. Wang, J. Xu, C.C. Liu, Improvement of amperometric biosensor performance for H₂O₂ detection based on bimetallic PtM (M = Ru, Au, and Ir) Nanoparticles, Int. J. Electrochem. 2012 (2012) 410846.

[45] R. Szamocki, A. Velichko, F. Mücklich, S. Reculusa, S. Ravaine, S. Neugebauer, W. Schuhmann, Improved enzyme immobilization for enhanced bioelectrocatalytic activity of porous electrodes, Electrochem. Commun. 9 (2007) 2121–2127.

[46] G. Sanzò, I. Taurino, R. Antiochia, L. Gorton, G. Favero, F. Mazzei, G. De Micheli, S. Carrara, Gold porous nanocorals obtained with bubble electrodeposition for enzymatic and non-enzymatic detection of glucose, Bioelectrochemistry 112 (2016) 125–131.

[47] I. Taurino, G. Sanzò, F. Mazzei, G. Favero, G. De Micheli, S. Carrara, Fast synthesis of platinum nanopetals and nanospheres for highly-sensitive non-enzymatic detection of glucose and selective sensing of ions, Sci. Rep. 5 (2015) 15277.

[48] S. Xiao, F. Xiao, Y. Hu, S. Yuan, S. Wang, L. Qian, Y. Liu, Hierarchical nanoporous gold-platinum with heterogeneous interfaces for methanol electrooxidation, Sci. Rep. 4 (2014) 4370.

[49] Y. Zhou, G. Yu, F. Chang, B. Hu, C.J. Zhong, Gold-platinum alloy nanowires as highly sensitive materials for electrochemical detection of hydrogen peroxide, Anal. Chim. Acta 757 (2012) 56–62.

[50] C. Li, H. Wang, Y. Yamauchi, Electrochemical deposition of mesoporous Pt-Au alloy films in aqueous surfactant solution: towards a highly sensitive amperometric glucose sensor, Chem. Eur. J. 19 (2013) 2242–2246.

[51] M.T. Sulak, Ö. Gökdoğan, A. Gülce, H. Gülce, Amperometric glucose biosensor based on gold-deposited polyvinylferrocene film on Pt electrode, Biosens. Bioelectron. 21 (2006) 1719–1726.

[52] J. Manso, M.L. Mena, P. Yáñez-Sedeño, J. Pingarrón, Electrochemical biosensors based on colloidal gold–carbon nanotubes composite electrodes, J. Electroanal. Chem. 603 (2007) 1–7.

[53] X. Guo, B. Liang, J. Jian, Y. Zhang, Xu. Ye, Glucose biosensor based on a platinum electrode modified with rhodium nanoparticles and with glucose oxidase immobilized on gold nanoparticles, Microchim. Acta 181 (2014) 519–525.

[54] X. Chu, D. Duan, G. Shen, R. Yu, Amperometric glucose biosensor based on electrodeposition of platinum nanoparticles onto covalently immobilized carbon nanotube electrode, Talanta 71 (2007) 2040–2047.

[55] X. Jiang, Y. Wu, X. Mao, X. Cui, L. Zhu, Amperometric glucose biosensor based on integration of glucose oxidase with platinum nanoparticles/ordered mesoporous carbon nanocomposite, Sensor. Actuat. B 153 (2011) 158–163.

[56] L.M. Fischer, M. Tenje, A.R. Heiskanen, N. Masuda, J. Castello, A. Bentien, J. Emnéus, J. Jakobson, A. Boisen, Gold cleaning methods for electrochemical detection applications, Microelectron. Eng. 86 (2009) 1282–1285.

[57] J.H. Han, S. Park, H. Boo, H.C. Kim, J. Nho, T.D. Chung, Solid-state reference electrode based on electrodeposited nanoporous platinum for microchip, Electroanalysis 19 (2007) 786–792.